



Published in final edited form as:

Nat Biomed Eng. 2020 November ; 4(11): 1053–1062. doi:10.1038/s41551-020-00606-8.

Gelling hypotonic polymer solution for extended topical drug delivery to the eye

Yoo Chun Kim^{1,2}, Matthew Shin^{1,2}, Sean Hackett², Henry T. Hsueh^{1,3}, Raquel Lima e Silva², Abhijit Date^{1,2,†}, Hyounkoo Han^{1,2}, Byung-Jin Kim², Amy Xiao^{1,4}, Youngwook Kim^{1,5}, Laolu Ogunnaike^{1,3}, Nicole M. Anders⁶, Avelina Hemingway⁶, Ping He⁶, Albert S. Jun², Peter J. McDonnell², Charles Eberhart², Ian Pitha², Donald J. Zack², Peter Campochiaro², Justin Hanes^{1,2,3,4,6,7,*}, Laura M. Ensign^{1,2,3,4,6,8,*}

¹Center for Nanomedicine at the Wilmer Eye Institute, Johns Hopkins University School of Medicine, Baltimore, MD 21231

²Department of Ophthalmology, Wilmer Eye Institute, Johns Hopkins University School of Medicine, Baltimore, MD 21287

³Department of Chemical & Biomolecular Engineering, Johns Hopkins University, Baltimore, MD 21218

⁴Department of Biomedical Engineering, Johns Hopkins University, Baltimore, MD, 21218

⁵Department of Biophysics, Johns Hopkins University, Baltimore, MD, 21218

⁶The Sidney Kimmel Comprehensive Cancer Center at Johns Hopkins University, Baltimore, MD 21287

⁷Departments of Pharmacology and Molecular Sciences and Neurosurgery, Johns Hopkins University, Baltimore, MD 21287

⁸Departments of Pharmacology and Molecular Sciences, Gynecology and Obstetrics, and Infectious Diseases, Johns Hopkins University, Baltimore, MD 21287

Abstract

Eye-drop formulations should hold as high a concentration of soluble drug in contact with ocular epithelium for as long as possible. However, eye tears and frequent blinking limit drug retention

Users may view, print, copy, and download text and data-mine the content in such documents, for the purposes of academic research, subject always to the full Conditions of use:http://www.nature.com/authors/editorial_policies/license.html#termsReprints and permissions information is available at www.nature.com/reprints.

*Correspondence and requests for materials should be addressed to, hanes@jhmi.edu; lensign@jhmi.edu.

Author contributions

Y.C.K., M.S., S.H., P.C., J.H. and L.E. designed experiments. Y.C.K., M.S., S.H., H.T.H., R.F., A.D., H.H., B.J.K., A.X., Y.K., L.O., N.M.A., A.H., P.H., C.E., I.P. performed experiments and/or analyzed experimental data. Y.C.K., M.S., S.H., B.J.K., N.M.A., J.H. and L.E. wrote sections of the manuscript. All authors read and approved the final version of the manuscript.

†Current address: The Daniel K. Inouye College of Pharmacy, University of Hawaii Hilo, 200 W. Kawili Street, Hilo, HI 96720

Data availability

The main data supporting the findings of this study are available within the paper and its Supplementary information. The associated raw data are too large to be readily shared publicly but are available from the corresponding author on reasonable request.

Competing interests

Y.C.K., A.D., L.E., and J.H. are inventors on patents/patent applications related to this technology.

Supplementary information is available for this paper at <https://doi.org/10.1038/s41551-01X-XXXX-X>.

on the ocular surface, and gelling drops typically form clumps that blur vision. Here, we describe a gelling hypotonic solution containing a low concentration of a thermosensitive triblock copolymer, for extended ocular drug delivery. On topical application, the hypotonic formulation forms a highly uniform and clear thin layer that conforms to the ocular surface and resists clearance from blinking, significantly increasing the intraocular absorption of hydrophilic and hydrophobic drugs and extending the drug–ocular-epithelium contact time with respect to conventional thermosensitive gelling formulations and commercial eye drops. We also show that the conformal gel layer allows for therapeutically relevant drug delivery to the eyeball's posterior segment in pigs. Our findings highlight the importance of formulations that conform to the ocular surface prior to viscosity enhancement, for increased and prolonged ocular-surface contact and drug absorption.

Eye drops are the dominant dosage form for the ocular route, and are used for a wide range of indications including glaucoma, dry eye, inflammation, infection, and allergy. However, as with all exposed epithelial surfaces, there are innate protective mechanisms that hinder efficient drug delivery to the eye. Tears continuously bathe the ocular surface before draining into the nasolacrimal duct, and the blinking of the eyelids frequently wipes the ocular surface clean of debris and excess fluids. Thus, only a small fraction of drugs administered by eye drops is typically absorbed into the eye¹, often necessitating multiple doses per day. As the number of eye drop doses per day increases, so does the potential for ocular surface irritation and systemic side effects, while patient compliance to the treatment regimen decreases². Approaches for achieving more efficient and longer-lasting topical ocular drug delivery are desperately needed.

To increase ocular drug absorption without disrupting the ocular epithelium, an eye drop formulation should hold as high concentration of soluble drug in contact with the tissue for as long as possible. Poorly soluble drugs are often formulated as milky suspensions, which can blur vision on application. For highly potent insoluble or poorly soluble drugs, solubility enhancers may be used, but these approaches still have the issue of limited retention on the ocular surface. Viscosity-enhancing polymers can increase retention time by resisting lacrimal drainage, though there is typically uneven coating that blurs vision and difficulty in dispensing single, reproducible volume drops from dropper bottles can be an issue. Ointments are also sometimes used, though they are messy and impact on vision typically limits to use at bedtime. Another option is *in situ* gelling systems, which are liquids that undergo a sol-gel transition triggered by temperature, polymerization, ions, or some other physical stimulus on application to the eye³. However, there are only a handful of eye drop products available that gel upon application, partly because immediate gelation upon contact with the ocular surface typically leads to clumpy gels that can also be messy and blur vision.

Preclinically, a variety of *in situ* gelling systems has been studied for topical ocular drug delivery, with thermosensitive polymers being one of the most extensively tested³. Here, we used Pluronic F127, a triblock copolymer that has thermoreversible gelling properties above the critical gel concentration (CGC) of about 15–16 % (w/w) at physiological conditions⁴. Pluronic F127 is an ingredient in a variety of FDA approved products,⁵ though at concentrations typically < 2% (w/w) in eye drops. The conventional approach for

formulating thermoreversible polymers for *in situ* gelation is to use polymer concentration above the CGC, such that a gel forms immediately as temperature increases past the sol-gel transition temperature^{3,4}. In contrast, our aqueous formulation contains F127 at a concentration below its CGC, such that it will not gel *in vitro*. This is particularly important for a polymer like F127, which has a sol-gel transition temperature in the range in which it may prematurely gel at room temperature⁴. The key to our formulation approach is that the polymer solution contains lower than physiological ion content, so it is hypotonic to the ocular surface and causes osmotically-induced water absorption upon application. Water absorption spreads and concentrates the polymer right at the ocular surface, resulting in a thin, uniform, clear gel that holds drug on the ocular surface and fits comfortably under the eyelids to resist clearance from blinking. In contrast, conventional thermogelling formulations, which are isotonic to the eye and contain polymer above the CGC, immediately form clumpy, uneven gels on contact with the eye, which may be wiped away by the eyelids, leading to suboptimal drug delivery. We demonstrate that our hypotonic, lower concentration thermogelling formulations out-perform both conventional isotonic thermogelling formulations and commercial eye drops for drugs that lower intraocular pressure, both hydrophilic (brimonidine tartrate) and hydrophobic (brinzolamide), as well as a hydrophobic peptide drug (cyclosporine) used for treating dry eye. Importantly, our hypotonic gelling formulation caused no signs of ocular irritation or toxicity with twice-daily administration for up to 5 weeks in rabbits as measured by corneal staining, blink rate test, and corneal histology. Further, characterization of the uniformity, refractive index, and absorbance suggest visual clarity would be maintained, and the shear-thinning properties are comparable to commercial lubricating eye drops. We further demonstrate data to support the hypothesis that by holding the drug in high concentration at the ocular surface, drug delivery to the posterior retina/choroid can be increased in large animals with eyes more similar in size to the human eye, leading to the prevention of laser-induced choroidal neovascularization.

Results

Hypotonicity leads to uniform surface coating and gelation.

In contrast to liquid eye drops, gels may reside longer on the ocular surface to provide increased intraocular drug absorption. The conventional formulation approach for thermoreversible polymer eye drops includes polymer at or above the CGC (~15–16% w/w for F127) in aqueous solution isotonic to the ocular surface (~290 mOsm/kg), where 18% F127 is commonly used in numerous prior topical eye drop studies⁶. Immediate gelation on contact would result in uneven, clumpy gels may be removed from the ocular surface by the eyelids, get caught up the lids and lashes, and obscure vision. We hypothesized that the potential advantages of a thermoreversible gel in terms of duration on the ocular surface could be better realized by creating a more uniform gel layer that would conform to the contours of the ocular surface and fit comfortably under the eyelids during blinking. Further, both the polymer concentration and tonicity could be lowered to allow for increased surface coverage and uniformity driven by water absorption that also acts to concentrate the polymer to gel on the ocular surface. We first sought to determine whether there must be a balance between the polymer dilution and the extent of water absorption that occurs to achieve

gelation on the ocular surface. Thus, we evaluated the pharmacodynamic effect of hypotonic eye drops containing one of two common ocular drugs with 10–18% F127. Reduction of intraocular pressure (IOP) after a single dose of brimonidine tartrate (BT), and tear production after a single dose of cyclosporine A (CsA) was measured over time in normotensive rabbits. For both drugs, there was an increase in cumulative drug effect going from 10% to 12% w/w F127, which then decreased as F127 concentration increased to 15% and 18% w/w (Supplementary Fig. 1a,b). This suggested that a concentration of 12% F127 effectively balanced polymer concentration with the extent of water absorption by the ocular tissues.

We then sought to visualize the eye drop behavior upon application *in vivo* using optical coherence tomography (OCT) imaging in rats. The hypotonic 12% F127 formulation (12% Hypo) was compared to an isotonic 12% F127 formulation (12% Iso), which should behave as a viscous liquid that does not induce water absorption by the ocular tissues, and a conventional isotonic 18% F127 formulation (18% Iso). The immediate gelation of the conventional 18% Iso formulation resulted in a thick, irregular coating on the ocular surface that was variable between animals (Supplementary Fig. 1c) and more readily cleared upon blinking (Fig. 1a, top row). In contrast, the 12% Hypo formulation formed uniform surface coatings that were consistent between animals (Supplementary Fig. 1d) and that persisted on the ocular surface after blinking (Fig. 1a, middle row). The 12% Iso formulation, which does not concentrate upon application to the eye to undergo a sol-gel transition, was cleared after blinking (Fig. 1a, bottom row). To visualize the macroscopic behavior of the formulations, F127 was fluorescently labeled (Supplementary Fig. 2a–d) (imparted blue color) and movies were taken to capture eye drop application to conscious rabbits. Fluorescent labeling and adjustment of salt content did not affect the F127 gelling transition temperature (T_{gel}) (Supplementary Fig. 2d). The immediate gelation of the conventional 18% Iso resulted in limited spreading and rapid clearance due to the blinking of the eyelids, which is also illustrated in the schematic representation to the left of the real-time recording in Supplementary Video 1. In contrast, the 12% Hypo formulation spread to coat the eye (Supplementary Video 1).

To visualize the residence time of the 12% Hypo formulation on the surface of the eye, fluorescently labeled F127 was again used. The 12% Hypo formulation was still clearly evident by fluorescent imaging of cryosections of the rat eye 3 h after administration, whereas the 12% Iso formulation was undetectable due to clearance by blinking (Supplementary Fig. 2f). We then sought to determine whether the prolonged residence time of the 12% Hypo formulation relative to the 12% Iso formulation was due to concentration of the polymer sufficient to cause gelation. As the 12% Hypo formulation cannot gel *in vitro*, the observation of the gelation phenomenon can only be performed after administration to an intact eye. To do this, we used real-time multiple particle tracking (MPT) to visualize the motion of fluorescent probe nanoparticles within the eye drop formulations *in vitro*, as well as on the surface of the eye of rats after administration *in vivo*. Nanoparticles diffuse freely within liquids due to thermal motion, and their diffusion rate, expressed here as the ensemble-averaged mean square displacement ($\langle MSD \rangle$) at a time scale of 1 s, is directly related to the viscosity and physical pore structure of the surrounding environment⁷. Thus, MPT facilitates rheological measurement on a micro-scale where

traditional bulk rheometric analysis is not feasible⁸. Here, we synthesized nanoparticles with non-adhesive surface coatings to ensure that any impact on nanoparticle mobility would reflect steric entrapment⁹. *In vitro* at 37°C, 200 nm nanoparticles were effectively trapped within the 18% Iso gel polymer micelle network, exhibited by the ~130-fold lower <MSD> compared to unobstructed nanoparticle diffusion in the viscous 12% Hypo and 12% Iso fluids (Fig. 1b). However, when the nanoparticles were administered in the 12% Hypo formulation to the intact eye *in vivo* and then visualized *ex vivo*, the nanoparticles exhibited a low <MSD> similar to nanoparticles administered in the 18% Iso formulation (Fig. 1b). In contrast, nanoparticles administered in the 12% Iso formulation diffused relatively unobstructed (Fig. 1b), demonstrating that a gel did not form *in vivo*. Representative *ex vivo* trajectories demonstrate the contrast between the nanoparticles sterically trapped within the gel formed on the ocular surface *in vivo* by 12% Hypo and 18% Iso compared to freely diffusive nanoparticles in the 12% Iso viscous liquid (Fig. 1c). As increasing the viscosity of the vehicle fluid is a common approach to increase residence time on the ocular surface¹⁰, we further compared the 12% Hypo formulation to 12% Iso. The *in vivo* gelation behavior of the 12% Hypo formulation led to prolonged levels of BT in rat ocular tissues (cornea, conjunctiva, aqueous humor) for at least 8 h after the last dose compared to the 12% Iso formulation (Supplementary Fig. 2g–i). Further, increased intraocular delivery of BT with the 12% Hypo formulation led to a sustained decrease in IOP in normotensive rabbits that was significantly lower than that of the 12% Iso formulation for at least 6–10 h (Supplementary Fig. 2j).

The hypotonic gel enhances intraocular drug absorption.

We then formulated several commonly used topical anterior segment drugs with different physicochemical properties (Supplementary Table 1) to compare ocular delivery in the 12% Hypo gelling formulation to the conventional gelling formulation approach (18% Iso) and the corresponding commercially available formulations. Brimonidine tartrate (BT) is commercially available as an aqueous solution at 0.15% w/v (Alphagan® P), and was readily soluble in the 12% Hypo and 18% Iso vehicles. We found that BT dissolved in the 12% Hypo formulation (12% Hypo(BT)) provided significantly higher drug concentration in the rat cornea at 1, 4, and 8 h after the last dose compared to 18% Iso(BT) and Alphagan® P (Fig. 2a). We observed a similar trend in the conjunctiva, although the increased drug concentration in the 12% Hypo(BT) group was only significant at 8 h (Fig. 2b). In the aqueous humor, the 12% Hypo(BT) formulation provided significantly increased drug concentration compared to 18% Iso(BT) at 4, and 8 h, and significantly increased drug concentration compared to Alphagan® P at 1, 4 and 8 h (Fig. 2c). We then evaluated each formulation for IOP reduction with a single dose in normotensive rabbits. The 12% Hypo(BT) formulation provided the largest and most sustained decrease in IOP, which was still significant compared to both the 18% Iso(BT) and Alphagan P at 10 h (Fig. 2d). As expected, the 12% Hypo vehicle (Vehicle) did not affect IOP (Fig. 2e). Surprisingly, despite the prolonged intraocular absorption provided by the 12% Hypo(BT) formulation compared to Alphagan® P, the systemic BT exposure after a single dose in rabbits was similar (Fig. 2f). Systemic drug absorption after topical dosing is a key factor that limits intraocular drug absorption³, and achieving the same efficacy with less frequent dosing would reduce overall systemic drug exposure and potential side effects. Indeed, equivalent efficacy with reduced

systemic exposure was the rationale for approval of Allergan's most recent iteration of brimonidine eye drops¹¹.

We next formulated two anterior segment drugs with relatively low water solubility, brinzolamide (BRZ) and cyclosporine A (CsA) (Supplementary Table 1). The commercial formulations for both drugs are milky suspensions, whereas the 12% Hypo formulations were both optically clear at the matched drug concentrations (1% w/v and 0.05% w/v, respectively) (Supplementary Fig. 3). Notably, both commercial formulations contain carbomer polymers commonly used for viscosity enhancement. We found that 12% Hypo(BRZ) provided significantly increased drug concentrations in rat cornea at 4 and 8 h after the last dose compared to 18% Iso(BRZ) and Azopt® (Fig. 3a). The trend was similar in the conjunctiva, but only significant at 4 h (Fig. 3b). In the aqueous humor, the drug concentrations were similar for all formulations (Fig. 3c), which is reflective of the low drug concentrations and lack of BRZ accumulation in the aqueous observed in humans¹². In normotensive rabbits, a single dose of 12% Hypo(BRZ) provided the largest and most sustained decrease in IOP, which was still significant compared to both the 18% Iso(BRZ) and Azopt® at 8 h (Fig. 3d). For CsA, we found that 12% Hypo(CsA) provided significantly increased drug concentrations in the rat cornea compared to 18% Iso(CsA) and Restasis® at 4 and 8 h after the last dose (Fig. 3e). The trend was similar in the conjunctiva, but only statistically significant at 4 h (Fig. 3f).

Enhanced delivery to the back of the eye in mice.

We next sought to determine whether providing enhanced intraocular drug absorption with the hypotonic gelling formulation would also provide therapeutically relevant drug delivery to the posterior segment. We formulated two water-soluble drugs with drastically different partition coefficients ($\log P$) (Supplementary Table 1), acriflavine hydrochloride (ACF) and sunitinib malate (SM), which have been demonstrated to have anti-angiogenic properties in the eye^{13,14}. As shown in Figure 4A, once-daily dosing with 0.5% ACF in the 12% Hypo formulation (12% Hypo(ACF)) resulted in significant suppression of laser-induced choroidal neovascularization (CNV) compared to the fellow eye treated with 12% Hypo vehicle only. In contrast, ACF dosed in water did not significantly suppress CNV compared to the fellow eye treated with the vehicle only (Supplementary Fig. 4a). Once-daily dosing of 0.4% SM in the 12% Hypo formulation (12% Hypo(SM)) also significantly suppressed laser-induced CNV compared to the fellow eye treated with the 12% Hypo vehicle only (Fig. 4a). However, SM dosed in saline did not significantly suppress CNV compared to the fellow eye treated with the vehicle only (Supplementary Fig. 4b).

It was surprising to observe increased delivery to the posterior segment using the 12% Hypo gel-forming vehicle, so we attempted to gain some mechanistic insight *in vitro*. Since SM is currently in clinical trials for treating wet age-related macular degeneration ([ClinicalTrials.gov NCT03953079](https://clinicaltrials.gov/ct2/show/study/NCT03953079)), we used it as our model drug moving forward. One major challenge for any *in vitro* characterization is that the 12% Hypo formulation will not form a gel at 37°C, and it is difficult to model the epithelial water absorption effect that concentrates the polymer to form a gel upon administration *in vivo*. Thus, we had to use 18% F127 to investigate the effect of the gel on corneal drug permeability and drug release.

Using excised rabbit cornea tissue, we found that the average apparent corneal permeability coefficient measured at 30 min for SM in F127 gel (18% Hypo(SM)) was not different than SM in Saline (Supplementary Fig. 5), which means the gel itself does not make the cornea inherently more permeable to the drug. However, others have reported similar or lower *in vitro* corneal permeability of drugs formulated as gels, micelles, or other types of sustained-release systems^{15,16}, likely because there is not an appropriate method for modeling the relative clearance *in vitro*. In other words, *in vitro* permeability often does not reflect the improvement in ocular drug delivery *in vivo*, especially when comparing an immediate release formulation (e.g. aqueous solution) to a sustained release formulation (e.g. 12% Hypo or 18% Iso). Indeed, SM release from F127 gel (18% Hypo(SM)) *in vitro* was prolonged compared to the viscous liquid (12% Iso(SM)) reflecting the sustained release of drug from gels compared to viscous liquids (Supplementary Fig. 6). While the formation of a gel did not significantly change SM permeability through corneal tissue *in vitro*, gels provide prolonged residence time and drug release on the ocular surface, which likely contributed to the increased intraocular drug absorption observed with the 12% Hypo formulation *in vivo*.

Enhanced delivery to the back of the eye in rabbits and pigs.

We next sought to test if the hypotonic gelling formulation can deliver therapeutically relevant drug concentrations to the posterior segment in larger animals with eyes that are more similar in size to human eyes¹⁷. We measured levels of both sunitinib and its major active metabolite, N-desethyl sunitinib, which has been shown to be similarly potent to sunitinib¹⁸. The combined concentrations of sunitinib and N-desethyl sunitinib in various ocular tissues are shown after daily dosing with 12% Hypo(SM) for 14 days in rabbits (Fig. 5a) and 5 days in pigs (Fig. 5b). Concentrations in the retina and choroid/retinal pigment epithelium (RPE) tissue homogenates were well above the K_i for SM inhibition of vascular endothelial growth factor receptor (VEGFR)/platelet derived growth factor receptor (PDGFR)¹⁹ in both rabbits (Fig. 5a) and pigs (Fig. 5b). However, sunitinib is known to bind to ocular melanin¹⁴, which reduces the amount of available drug. Thus, we then tested whether the potentially therapeutically relevant level of drug in the posterior tissues may provide suppression of neovascularization in pigs. Once-daily dosing with 12% Hypo(SM) resulted in significant suppression of laser-induced CNV compared to dosing with the same concentration of SM formulated in saline (SM in Saline) or dosing with 12% Hypo vehicle (Vehicle) alone (Fig. 5c).

Compatibility with the ocular surface and visual acuity.

We next evaluated the effect of chronic topical administration of the hypotonic gelling formulation vehicle in rabbits. Rabbits were dosed two times per day for 5 weeks, and the 12% Hypo formulation was compared to the 12% Iso vehicle, commercially available balanced salt solution (BSS), and no treatment (Untreated). For all the treatment groups, no significant differences in corneal staining and blinking frequency were observed compared with untreated rabbits (Fig. 6a,b). Similarly, no significant histological differences were observed in corneas obtained at the end of the 5 weeks of treatment across all groups (Fig. 6c).

Since the hypotonic gelling formulation has a prolonged residence time on the ocular surface, we sought to evaluate material properties relevant to the potential impact on vision and comfort. We found no significant differences in the visual light absorbance of F127 solution and gel compared to water at 37°C (Supplementary Fig. 7a). Similarly, the refractive index of F127 solution and gel was between that of human tear fluid²⁰ and common soft contact lens materials²¹ (Supplementary Fig. 7b). Further, F127 gel showed significant shear thinning (lubricating) behavior, which is necessary for ocular comfort when blinking. The viscosity of F127 gel at high shear rates was similar to that of commercially available lubricating eye gel (GenTeal® Severe Dry Eye Relief Lubricant Eye Gel) (Supplementary Fig. 8a,b).

Discussion

Over 90% of ophthalmic products are eye drops²². However, despite the non-invasive administration and relative simplicity of eye drops, there is significant room for improvement. Low intraocular drug absorption, rapid clearance, intensive dosing regimens, and ocular surface toxicity resulting from repeated administration contribute to poor patient adherence and even discontinuation of medication²³. These limitations can be especially problematic for chronic diseases, such as dry eye and glaucoma. Numerous glaucoma medications, including BT and BRZ, require dosing up to three times per day, increasing the risk of side effects²⁴. Further, adherence rates for eye drops that require dosing more than two times a day are as low as 39%²⁵. Eye drops can only effectively treat disease when used properly, which for glaucoma, poor adherence means uncontrolled IOP and higher rates of visual loss²⁶.

Here, we describe an approach to utilize thermosensitive gelling polymers as eye drops that provide increased and sustained intraocular drug absorption without increased systemic drug exposure. Further, the eye drop vehicle was compatible with a variety of ophthalmic drugs with different physicochemical properties, suggesting potential for broad versatility. Key features for tailoring the formulation for maximal compatibility with the unique physiological properties of the ocular surface were hypotonicity and polymer concentration below the CGC. Upon application, the eye drop spread uniformly over the surface of the eye, while water absorption concentrated the polymer at the ocular surface to form a thin, clear gel layer that was resistant to clearance from blinking. The conventional approach for increasing the residence time of drugs on the ocular surface is the use of excipients, including cellulose derivatives, hyaluronan, polycarbophil, and carbopol that provide viscosity enhancement and/or mucoadhesion¹⁰. One of the few examples of a commercially available *in situ* gelling eye drop, Timoptic-XE®, contains gellan gum, which undergoes a gel transition when exposed to cations in the tear film³. Timoptic XE® was shown to provide similar efficacy in lowering IOP with once-daily administration compared to twice-daily administration of timolol solution²⁷. However, significantly more patients reported blurred vision and tearing with the gel-forming eye drop compared to the solution eye drop²⁸. In contrast, we describe here a thin, uniform, clear gel with similar absorbance and refractive index as water or contact lens materials that is not expected to negatively impact vision^{21,29,30}. It is possible that formulating other viscosity-enhancing and gel-forming

materials hypotonically with lower polymer concentration may further increase residence time and reduce vision distortion in a similar manner.

Drugs are typically delivered to the posterior segment via injections, such as intravitreal injection of anti-VEGF biologics. While injections are performed routinely, there is a small but significant risk for serious adverse events that endanger the patient's vision³¹. Further, treatment may require returning to the clinic every 4–8 weeks to achieve the best visual outcome³². Eye drops for treating retinal diseases could potentially be safer, simpler, and cheaper. However, efforts toward clinical development have not been successful. One potential factor is that drugs that perform well in preclinical rodent studies may not be as effective in humans due to the large size difference between human and rodent eyes^{33–38}. Thus, larger animals such as rabbits, pigs, or non-human primates are needed to assess whether similar drug biodistribution can be achieved in larger eyes. For example, topical administration of pazopanib 3x per day successfully suppressed retinal vascular leakage in mice, but 4x per day topical dosing failed to show efficacy in a rabbit model³⁹.

Efficacy in reducing the prevalence of grade IV lesions in a primate laser CNV model was demonstrated with topical administration of regorafenib suspension,⁴⁰ leading to a phase 2 clinical trial that failed due to inadequate efficacy⁴¹. It was later reported that levels of regorafenib and pazopanib in the posterior tissues were quite low after topical dosing in monkeys, and that the levels in both monkeys and rabbits were much lower than in rats⁴². They went on to show that processing the regorafenib suspension such that the particulates were nano-sized rather than micron-sized could improve delivery to the posterior segment in rabbits⁴². Another formulation approach that has shown promise for insoluble drugs is complexation with cyclodextrins, which provided delivery of dexamethasone to the retina in rabbits⁴³ that translated to efficacy similar to subtenon triamcinolone in a clinical trial for treating diabetic macular edema⁴⁴.

Here, enhanced drug delivery to the posterior segment of the eye was an unexpected finding. We achieved robust ocular biodistribution of water-soluble sunitinib malate (SM) with daily topical delivery in both rabbits and pigs, which have similar corneal^{35,45,46} and scleral thickness^{47–49}, and vitreous volume^{33,50} compared to the human eye. We speculate that holding the drug in contact with the ocular surface for longer periods of time can result in increased drug delivery to the posterior segment, though the efficiency of delivery to the posterior tissues is likely to be dependent on individual drug properties, such as solubility and log *P*. The drug distribution in rabbits and pigs shown in Figure 5 showed higher levels in the cornea/conjunctiva and retina/choroid/RPE with lower levels in the vitreous, suggesting enhanced delivery may occur through transscleral diffusion and/or uveoscleral outflow. We demonstrated that the daily administration of 12% Hypo(SM) effectively prevented laser-induced CNV in both rodents and pigs. A daily eye drop that could potentially delay the time between clinic visits, or even replace intravitreal injections, may improve patient quality of life. We also anticipate that absorption-induced gelation can be applied more broadly to other absorptive mucosal tissues, such as the nasal⁵¹, vaginal⁵², and gastrointestinal epithelia^{53,54}.

Methods

Materials.

Lutrol F127 (F127), tetrahydrofuran (THF), carbonyldiimidazole (CDI), BRZ, Span 20, dimethylsulfoxide, FITC-labeled Griffonia simplicifolia (GSA) lectin, and GSA isolectin B4 conjugated with Dylight 594 were purchased from Vector Laboratories. Fluorescent carboxyl-modified yellow-green polystyrene nanoparticles (200 nm), Hoechst trihydrochloride, and lissamine green were purchased from Sigma-Aldrich. BT was purchased from Cayman chemical. CsA was purchased from Carbosynth. ACF was purchased from TCI chemical. SM was purchased from LC laboratories. Brimonidine-d4, brinzolamide-d5, sunitinib-d10, and cyclosporine A-¹⁵N₁₁ were purchased from Toronto Research Chemicals. Amine-modified PEG (5 kDa) was purchased from Creative PEGworks. Regenerated cellulose dialysis membrane with 1 kDa and 10 kDa MW cut-off was purchased from Spectrum Labs. Normal goat serum, phosphate buffered saline (PBS), and 4% paraformaldehyde were purchased from Thermo Fisher Scientific. Optimal Cutting Temperature (OCT) embedding medium was purchased from Fisher Scientific. Alphagan and Restasis was purchased from Allergan. Azopt was purchased from Alcon. A Franz cell was purchased from the PermeGear. Excised rabbit eyes were purchased from Pel-freez Biological.

Eye drop formulations.

To make hypotonic F127 solution ranging from 12–20% (w/w), F127 powder was added to water using indicated weight ratios and stored at 4 °C until fully dissolved. For the hypotonic BT formulations, BT powder was weighed and dissolved into hypotonically prepared 12 – 18% (w/w) of F127 to the final BT concentration of 0.15% (w/v). To make hypotonic BRZ formulations, 4 mg BRZ, 0.02 mg of Span 20, and 0.0068 mg F127 were dissolved in 1.1 mL of acetone. After completely dissolving the materials, 0.4 mL of water was added. Acetone was evaporated using rotary evaporator and an additional amount of F127 powder was added to make 10 – 18% (w/w) of F127 at a BRZ concentration of 1% (w/v). To prepare hypotonic CsA formulations, 20 mg of cyclosporine A and 200 mg of F127 powder were added into 4 mL of dimethylsulfoxide. The obtained solution was then dialyzed in water with regenerated cellulose dialysis membrane with 1 kDa MW cut off for overnight at room temperature and stirred in DI water for 12 h. Additional water and F127 powder was added to achieve a final CsA concentration at 0.05% (w/v) in F127 solutions with final concentration ranging from 12–18% (w/w). In order to prepare 12% Hypo(ACF), ACF was dissolved (0.5% w/v) in 12% (w/w) F127 dissolved in DI water. To prepare ACF in Water, ACF was dissolved in DI water. To prepare 12% Hypo(SM) solution, SM was first dissolved in water at 1% (w/v) using an ultrasonic probe sonicator (Sonics). The prepared solution was then mixed with 20% (w/w) F127 in DI water at 4:6 ratio (w/w) to make the final solution with 0.4% (w/v) SM in 12% (w/w) F127. To prepare SM in Saline solution, SM was dissolved in sterile normal saline at a concentration of 0.4% (w/v) using an ultrasonic probe sonicator. For the BT, BRZ, and CsA formulations, pH was tested using pH strips (VWR Chemicals) and adjusted, if necessary, using 10 M NaOH (< 1% total volume) to reach pH 7 ± 0.5. To prepare isotonic F127 solutions, tonicity of the hypotonically prepared samples were adjusted by adding concentrated (up to 100-fold) BSS. Concentrated

BSS was prepared by lyophilizing the commercial formulation and re-dissolving it in water. The pH of SM and ACF formulations were measured using pH probe (Thermo Fisher Scientific). The osmolarity of the formulations (Supplementary Table 2) was measured using a vapor pressure osmometer (Wescor). For the measurements that were below the linear calibration range (100–1000 mOsm/kg), samples were mixed with an equal volume of BSS (300 ± 10 mOsm/kg) prior to the measurement. The measured mixture osmolality was used to calculate the sample osmolality by assuming a linear contribution from each component in the mixture.

Nanoparticle PEGylation.

Commercially available fluorescent nanoparticles (2% w/v) were densely coated with polyethylene glycol (PEG) to render the surface non-adhesive for probing local environmental microstructure as previously described⁹. Briefly, yellow-green fluorescent carboxyl-modified polystyrene nanoparticles (200 nm) were reacted with amine-modified PEG (5 kDa) via 1-ethyl-3-(3-dimethylaminopropyl)-carbodiimide coupling reaction as previously described⁵⁵. Particle size and ζ -potential were measured using a Zetasizer Nano ZS90 (Malvern Instruments). Particle size in water was measured at a scattering angle of 173° before (261 ± 8 nm) and after (290 ± 16 nm) PEGylation at the concentration of 0.1% (w/v). ζ -potential (0.02% (w/v) in 10 mM NaCl) was also measured before (-48 ± 7 mV) and after (-3 ± 2 mV) PEGylation to confirm successful conjugation of PEG to the free carboxylic acid groups on the nanoparticle surface⁹.

Multiple particle tracking.

For the *in vitro* multiple particle tracking, 30 μ L of the F127 solution was placed in a custom-made well chamber and 0.5 μ L of fluorescently-labeled PEGylated nanoparticles (0.02 mg/mL) were added. A coverslip was placed on top of the well and sealed with super glue to prevent evaporation and movement of the placed coverslip. The slides were then incubated in a temperature-controlled chamber enclosing the microscope for 15 min at 37°C . The slide was placed on an inverted epifluorescence microscope (Axio Observer D1; Carl Zeiss) and imaged with a $100\times/1.46$ N.A. oil-immersion objective. Videos of nanoparticle motion were recorded over 20 s at an exposure time of 66.7 ms by an Evolve 512 EMCCD camera (Photometrics). Obtained videos were analyzed using in-house code (MATLAB, MathWorks). The x, y coordinates of hundreds of nanoparticles centroids were identified and tracked over time (example nanoparticle trajectories shown in Fig. 1C) to calculate individual particle mean square displacement (MSD). The ensemble averaged MSD ($\langle\text{MSD}\rangle$) was calculated as the geometric mean of individual particle MSDs at a timescale of 1 s.

Animal studies.

Animal welfare statement.—All experimental protocols were approved by the Johns Hopkins Animal Care and Use Committee. All animals were handled and treated in accordance with the Association for Research in Vision and Ophthalmology (ARVO) Statement for Use of Animals in Ophthalmic and Vision Research. A specific sex was not specified when ordering any species, and roughly equivalent numbers of both male and

female animals were used. C57BL/6 mice, Sprague Dawley rats, New Zealand White rabbits, and Dutch Belted rabbits were obtained from Charles River. Yorkshire pigs were obtained from Archer Farm. Animals were anesthetized prior to euthanasia.

Optical coherence tomography imaging.—Corneal clearance of various formulations after blinking was determined by real-time *in vivo* imaging using the spectral domain optical coherence tomography (SD-OCT). Sprague Dawley rats were anesthetized and placed in a holding cylinder for stable image acquisition. Each image acquisition was processed with Envisu XHR 4110 ophthalmic imaging system (Leica Microsystems Inc.) with 10 mm telecentric lens. All images were obtained using a rectangular scanning mode (3 mm × 3 mm, 1000 A-scans × 100 B-scans, and 1.4 × 0.78 μm pixel size). After topical administration of a single eye drop (5 μL) of various formulations (12% Hypo, 12% Iso, 18% Iso), all images were obtained within 1 min and also immediately after each manual blinking the eyelids twice.

In vivo multiple particle tracking.—For the *in vivo* MPT, non-adhesive nanoparticles (0.0004% w/v) were added to 12% Hypo, 12% Iso, and 18% Iso formulations. Sprague Dawley rats were anesthetized prior to administering as an eye drop (5 μL). After 1 min, rats were euthanized by cervical dislocation and the eyes were immediately enucleated, taking care not to perturb the ocular surface. All the following procedures were done in the environmental chamber heated and humidified at 37°C. Surgical tools were pre-heated prior to starting of the experiment. Excised eyes were placed in a custom-made microwell on a glass cover slide with the cornea facing down towards the optical side of the inverted microscope. A custom-made cap was placed above the eye and sealed with superglue to prevent evaporation. Imaging was started within 2 min after sacrifice. Particles on the ocular surface were imaged and particle motion characterized as described above.

Pharmacokinetics studies.—Sprague Dawley rats 6–8 weeks of age were anesthetized using isoflurane. Eye drops (5 μL) in various formulations were delivered unilaterally, and the rats were placed back in an isoflurane chamber for an additional 5 min before allowing them to awaken. Eye drops were delivered twice per day for five days. After the last dose, rats were sacrificed 1, 4, and 8 h time points after the last treatment. While anesthesia was used to reduce variability in dosing between rats, the lack of reflexive blinking response would also mean reduced clearance in the initial minutes after dosing. Dosing of large animals was conducted without anesthesia to better recapitulate eye drop dosing in humans. Dutch Belted rabbits (2–3 kg, n = 6) were given 12% Hypo(SM) eye drops (50 μL) unilaterally once per day while gently restrained for a total of 14 days. Various ocular tissues were obtained 6 h after the last dose. Yorkshire pigs (20–30 kg, n = 4) were gently restrained and fed dried fruit as a distraction in order to unilaterally dose 12% Hypo (SM) daily (~50–100 μL approximate drop volume dosed with a commercially available eye dropper bottle) for 5 days. Various ocular tissues were obtained 1 h after the last dose. The reported K_i value for SM inhibition of VEGFR and PDGFR (~8–9 nM)¹⁹ was converted from molar concentration to mass concentration (~3.5 ng/mL) by assuming tissue density of 1 g/mL. Measurements of drug concentrations were conducted by liquid chromatography-tandem mass spectrometry (LC-MS/MS) as described in the supplementary methods.

IOP measurements.—For the IOP measurements in a normotensive rabbit model, New Zealand White rabbits (2 – 3 kg) were used. IOP was measured with a hand-held rebound tonometer (TonoVet) in the awake and lightly restrained rabbit. Each rabbit was acclimatized to the IOP measurement procedure for at least 5 days to obtain a stable background IOP reading. Average IOP measurements for an individual eye was measured every other day for 6 days (3 times total) and used as a baseline value. After single topical administration (50 μ L), IOP was measured every 2 h and change in IOP from the baseline (IOP) was reported.

Laser-induced choroidal neovascularization (CNV) studies.—*C57BL/6* mice (4 – 6 weeks) were anesthetized and the pupils were dilated with 1% tropicamide and 2.5% phenylephrine. A cover slip was placed on the cornea. A portable diode laser with a slit lamp delivery system was used to rupture Bruch’s membrane in 3 locations using a 75 μ m spot size, 0.1 s duration, and 150 mW power. Immediately after laser-induced rupture and each morning for the following six days, 5 μ L drug-containing (0.5% acriflavine hydrochloride or 0.4% sunitinib malate) eye drops were dosed to the treated eye and the contralateral eye was treated with the same volume of vehicle (12% Hypo, water, or saline, as denoted in the figures). The following morning (seven days after rupture of Bruch’s membrane), the mice were euthanized and the eyecups were fixed, stained with FITC-labeled GSA, and flat mounted. The area of CNV at each Bruch’s membrane rupture site was measured by a masked observer using Image Pro Plus. The area of CNV at the 3 rupture sites in one eye was averaged to give one experimental value for each eye.

Yorkshire pigs (20 – 30 kg, n = 4) were gently restrained and fed dried fruit as a distraction in order to bilaterally dose 0.4% sunitinib malate in 12% Hypo(SM) (n = 2), 0.4% sunitinib malate in saline (n = 1), or 12% Hypo vehicle (n = 1) daily (~50 – 100 μ L approximate drop volume dosed with an eye dropper bottle). Pigs were dosed daily for five days. On the sixth day, pigs were anesthetized and the pupils were dilated with 1% tropicamide and 2.5% phenylephrine and sterilized with a drop of 1% povidone. A fundus contact lens was placed on the cornea. A portable diode laser with a slit lamp delivery system was used to rupture Bruch’s membrane in 9 – 11 locations equidistant from the disc using a 75 μ m spot size, 0.1 s duration, and 430 mW power in each eye. The pig was then given another bilateral topical dose and kept warm with blankets until recovering from anesthesia. Topical eye drops were dosed bilaterally daily for an additional nine days using gentle restraint and food as a distraction. The next day after the last dose (ten days after rupture of Bruch’s membrane), pigs were euthanized, and the choroid was fixed, stained with FITC-labeled GSA, and flat mounted. The area of CNV at each Bruch’s membrane rupture site was measured by a masked observer using Image Pro Plus. Statistical analysis was performed using linear mixed model with each laser-induced CNV spot as a separate experimental value.

Safety study.—Topical eye drops (12% Hypo, 12% Iso, or BSS) were given to New Zealand White rabbits (n = 3) twice a day (8 h apart) for 5 weeks. Eye drops were given bilaterally, but each rabbit was given a different treatment in each eye (n = 3 eyes per group). At the end of each week, corneal staining and blink rates were assessed. These measures are used both preclinically and clinically to establish potential for ocular surface irritation/toxicity^{56,57}. For the blink rate measurements, rabbits were mildly restrained using a towel

and placed in a small container. The blinking rate was determined by counting the number of blinks in a 3 min period. All the blink rate measurements were done 3 h after the topical administration. Following the blinking rate measurement, the corneal staining test was performed. A single eye drop of lissamine green (1% in sterile saline) was topically administered, and corneal staining was scored using a previously reported grading scheme⁵⁸ by a board-certified ophthalmologist in a masked manner. For the histological evaluation, the eyes were enucleated and placed in 4% paraformaldehyde prior to paraffin embedding, sectioning, and H&E staining by the Johns Hopkins Reference Histology Laboratory. Histological sections were evaluated by a board-certified ophthalmic pathologist in a masked manner for the signs of inflammation and ocular surface damage.

Statistical Analysis.

Statistical analyses of two groups were conducted using two-tailed Student's t-test or two-tailed Mann-Whitney test or two-way analysis of variance (ANOVA). For the comparison of multiple groups, one-way ANOVA with Dunnett's multiple comparison test was done. Statistical analysis was done using GraphPad Prism 8. For the statistical analysis in the CNV model in pigs, we checked for the potential correlation among measurements of CNV size from the same eye and the correlation among the measurements from different eyes but the same animal were analyzed using linear mixed effects models with random intercepts at the level of eye and the level of animal. The intra-class correlation coefficients were close to zero, indicating low correlation among the measurements and therefore, the linear regression model was used and each CNV measurement was treated as an independent sample. Differences were considered to be statistically significant at a level of $p < 0.05$.

Reporting summary.

Further information on research design is available in the Nature Research Reporting Summary linked to this article.

Supplementary Material

Refer to Web version on PubMed Central for supplementary material.

Acknowledgements

The authors thank David Guyton for sharing his expertise in light refraction, Florin Selaru and Ling Li for assistance with the swine animal protocol, and the veterinary and husbandry staff for their assistance. This work was supported by the National Institutes of Health (R01EB016121, R01EY026578 and P30EY001765), the Robert H. Smith Family Foundation, a Sybil B. Harrington Special Scholar Award and a departmental grant from Research to Prevent Blindness, the KKESH - WEI Collaborative Research Fund, and a Hartwell Foundation Postdoctoral Fellowship. Drug measurements were conducted by the Analytical Pharmacology Core (APC) of the Sidney Kimmel Comprehensive Cancer Center at Johns Hopkins. The work conducted by the APC was supported by NIH grants P30CA006973 and S10OD020091, as well as grant number UL1TR001079 from the National Center for Advancing Translational Sciences (NCATS), a component of the National Institutes of Health (NIH), and the NIH Roadmap for Medical Research. Its contents are solely the responsibility of the authors and do not necessarily represent the official view of the NCATS or NIH.

References

1. Urtti A, Pipkin JD, Rork G & Repta AJ Controlled Drug Delivery Devices for Experimental Ocular Studies with Timolol .1. Invitro Release Studies. *Int J Pharm* 61, 235–240, doi:Doi 10.1016/0378-5173(90)90214-O (1990).
2. Hermann MM, Papaconstantinou D, Muether PS, Georgopoulos G & Diestelhorst M Adherence with brimonidine in patients with glaucoma aware and not aware of electronic monitoring. *Acta Ophthalmol* 89, E300–E305, doi:10.1111/j.1755-3768.2010.02050.x (2011). [PubMed: 21106046]
3. Agrawal AK, Das M & Jain S In situ gel systems as ‘smart’ carriers for sustained ocular drug delivery. *Expert Opin Drug Del* 9, 383–402, doi:10.1517/17425247.2012.665367 (2012).
4. Dumortier G, Grossiord JL, Agnely F & Chaumeil JC A review of poloxamer 407 pharmaceutical and pharmacological characteristics. *Pharm Res* 23, 2709–2728, doi:10.1007/s11095-006-9104-4 (2006). [PubMed: 17096184]
5. Rowe RC, Sheskey PJ, Owen S. n. C. & American Pharmacists Association. Handbook of pharmaceutical excipients / edited by Rowe Raymond C., Sheskey Paul J., Quinn Marian E.. 6th edn, (APhA/Pharmaceutical Press;, 2009).
6. Escobar-Chavez JJ et al. Applications of thermo-reversible pluronic F-127 gels in pharmaceutical formulations. *J Pharm Pharm Sci* 9, 339–358 (2006). [PubMed: 17207417]
7. Schuster BS, Ensign LM, Allan DB, Suk JS & Hanes J Particle tracking in drug and gene delivery research: State-of-the-art applications and methods. *Advanced drug delivery reviews* 91, 70–91, doi:10.1016/j.addr.2015.03.017 (2015). [PubMed: 25858664]
8. Squires TM & Mason TG Fluid Mechanics of Microrheology. *Annual Review of Fluid Mechanics* 42, 413–438, doi:10.1146/annurev-fluid-121108-145608 (2010).
9. Ensign LM, Schneider C, Suk JS, Cone R & Hanes J Mucus penetrating nanoparticles: biophysical tool and method of drug and gene delivery. *Adv Mater* 24, 3887–3894 (2012). [PubMed: 22988559]
10. Zignani M, Tabatabay C & Gurny R Topical semi-solid drug delivery: kinetics and tolerance of ophthalmic hydrogels. *Adv Drug Deliver Rev* 16, 51–60, doi:10.1016/0169-409X(95)00015-Y (1995).
11. Cantor LB Brimonidine in the treatment of glaucoma and ocular hypertension. *Ther Clin Risk Manag* 2, 337–346, doi:10.2147/tcrm.2006.2.4.337 (2006). [PubMed: 18360646]
12. Pharmacology/Toxicology NDA Review And Evaluation Simbrinza (NDA204251). (6 19, 2012).
13. Hackett SF et al. Sustained delivery of acriflavine from the suprachoroidal space provides long term suppression of choroidal neovascularization. *Biomaterials* 243, 119935, doi:10.1016/j.biomaterials.2020.119935 (2020). [PubMed: 32172031]
14. Tsujinaka H et al. Sustained treatment of retinal vascular diseases with self-aggregating sunitinib microparticles. *Nat Commun* 11, 694, doi:10.1038/s41467-020-14340-x (2020). [PubMed: 32019921]
15. Fathalla MA, Z. et al. Poloxamer-based thermoresponsive ketorolac tromethamine in situ gel preparations: Design, characterisation, toxicity and transcorneal permeation studies. *European Journal of Pharmaceutics and Biopharmaceutics* 114, 119–134, doi:10.1016/j.ejpb.2017.01.008 (2017). [PubMed: 28126392]
16. Abdelkader H, Ismail S, Kamal A & Alany RG Design and evaluation of controlled-release niosomes and discomes for naltrexone hydrochloride ocular delivery. *J Pharm Sci* 100, 1833–1846, doi:10.1002/jps.22422 (2011). [PubMed: 21246556]
17. Rodrigues GA et al. Topical Drug Delivery to the Posterior Segment of the Eye: Addressing the Challenge of Preclinical to Clinical Translation. *Pharm Res* 35, 245, doi:10.1007/s11095-018-2519-x (2018). [PubMed: 30374744]
18. Goodman VL et al. Approval summary: sunitinib for the treatment of imatinib refractory or intolerant gastrointestinal stromal tumors and advanced renal cell carcinoma. *Clin Cancer Res* 13, 1367–1373, doi:10.1158/1078-0432.CCR-06-2328 (2007). [PubMed: 17332278]
19. Roskoski R Jr. Sunitinib: a VEGF and PDGF receptor protein kinase and angiogenesis inhibitor. *Biochem Biophys Res Commun* 356, 323–328, doi:10.1016/j.bbrc.2007.02.156 (2007). [PubMed: 17367763]

20. Craig JP, Simmons PA, Patel S & Tomlinson A Refractive index and osmolality of human tears. *Optom Vis Sci* 72, 718–724 (1995). [PubMed: 8570161]
21. Gonzalez-Mejjome JM et al. Refractive index and equilibrium water content of conventional and silicone hydrogel contact lenses. *Ophthalmic Physiol Opt* 26, 57–64, doi:10.1111/j.1475-1313.2005.00342.x (2006). [PubMed: 16390483]
22. Patel A, Cholkar K, Agrahari V & Mitra AK Ocular drug delivery systems: An overview. *World J Pharmacol* 2, 47–64, doi:10.5497/wjp.v2.i2.47 (2013). [PubMed: 25590022]
23. Deokule S, Sadiq S & Shah S Chronic open angle glaucoma: patient awareness of the nature of the disease, topical medication, compliance and the prevalence of systemic symptoms. *Ophthal Physl Opt* 24, 9–15, doi:DOI 10.1046/j.1475-1313.2003.00155.x (2004).
24. Inoue K Managing adverse effects of glaucoma medications. *Clin Ophthalmol* 8, 903–913, doi:10.2147/OPTH.S44708 (2014). [PubMed: 24872675]
25. Schwartz GF & Quigley HA Adherence and persistence with glaucoma therapy. *Surv Ophthalmol* 53 Suppl1, S57–68, doi:10.1016/j.survophthal.2008.08.002 (2008). [PubMed: 19038625]
26. Stewart WC, Chorak RP, Hunt HH & Sethuraman G Factors associated with visual loss in patients with advanced glaucomatous changes in the optic nerve head. *Am J Ophthalmol* 116, 176–181, doi:10.1016/s0002-9394(14)71282-6 (1993). [PubMed: 8352302]
27. Shedden A, Laurence J, Tipping R & Timoptic XESG Efficacy and tolerability of timolol maleate ophthalmic gel-forming solution versus timolol ophthalmic solution in adults with open-angle glaucoma or ocular hypertension: a six-month, double-masked, multicenter study. *Clin Ther* 23, 440–450 (2001). [PubMed: 11318078]
28. Walters TR et al. Efficacy and tolerability of 0.5% timolol maleate ophthalmic gel-forming solution QD compared with 0.5% levobunolol hydrochloride BID in patients with open-angle glaucoma or ocular hypertension. *Clinical Therapeutics* 20, 1170–1178, doi:10.1016/S0149-2918(98)80112-4 (1998). [PubMed: 9916610]
29. Lira M, Pereira C, Real Oliveira ME & Castanheira EM Importance of contact lens power and thickness in oxygen transmissibility. *Cont Lens Anterior Eye* 38, 120–126, doi:10.1016/S0149-2918(98)80112-4 (2015). [PubMed: 25554499]
30. Olsen T On the calculation of power from curvature of the cornea. *Br J Ophthalmol* 70, 152–154, doi:10.1136/bjo.70.2.152 (1986). [PubMed: 3947615]
31. Jager RD, Aiello LP, Patel SC & Cunningham ET Jr. Risks of intravitreal injection: a comprehensive review. *Retina* 24, 676–698 (2004). [PubMed: 15492621]
32. Singer MA et al. HORIZON: an open-label extension trial of ranibizumab for choroidal neovascularization secondary to age-related macular degeneration. *Ophthalmology* 119, 1175–1183 (2012). [PubMed: 22306121]
33. Friedrich S, Cheng YL & Saville B Drug distribution in the vitreous humor of the human eye: The effects of intravitreal injection position and volume. *Current Eye Research* 16, 663–669, doi:DOI 10.1076/ceyr.16.7.663.5061 (1997). [PubMed: 9222083]
34. Kaplan HJ, Chiang CW, Chen J & Song SK Vitreous Volume of the Mouse Measured by Quantitative High-Resolution MRI. *Invest Ophth Vis Sci* 51 (2010).
35. Doughty MJ & Zaman ML Human corneal thickness and its impact on intraocular pressure measures: a review and meta-analysis approach. *Surv Ophthalmol* 44, 367–408 (2000). [PubMed: 10734239]
36. Zhang H et al. The measurement of corneal thickness from center to limbus in vivo in C57BL/6 and BALB/c mice using two-photon imaging. *Exp Eye Res* 115, 255–262, doi:10.1016/j.exer.2013.07.025 (2013). [PubMed: 23920154]
37. Park H et al. Assessment of axial length measurements in mouse eyes. *Optom Vis Sci* 89, 296–303, doi:10.1097/OPX.0b013e31824529e5 (2012). [PubMed: 22246334]
38. Bekerman I, Gottlieb P & Vaiman M Variations in eyeball diameters of the healthy adults. *J Ophthalmol* 2014, 503645, doi:10.1155/2014/503645 (2014). [PubMed: 25431659]
39. Iwase T et al. Topical pazopanib blocks VEGF-induced vascular leakage and neovascularization in the mouse retina but is ineffective in the rabbit. *Invest Ophthalmol Vis Sci* 54, 503–511, doi:10.1167/iovs.12-10473 (2013). [PubMed: 23169884]

40. Boettger MK, Klar J, Richter A & von Degenfeld G Topically administered regorafenib eye drops inhibit grade IV lesions in the non-human primate laser CNV model. *Invest Ophth Vis Sci* 56 (2015).
41. Jousseaume AM et al. The Developing Regorafenib Eye drops for neovascular Age-related Macular degeneration (DREAM) study: an open-label phase II trial. *Brit J Clin Pharmacol* 85, 347–355, doi:10.1111/bcp.13794 (2019).
42. Horita S et al. Species differences in ocular pharmacokinetics and pharmacological activities of regorafenib and pazopanib eye-drops among rats, rabbits and monkeys. *Pharmacol Res Persp* 7, e00545, doi:10.1002/prp2.545 (2019).
43. Loftsson T, Hreinsdottir D & Stefansson E Cyclodextrin microparticles for drug delivery to the posterior segment of the eye: aqueous dexamethasone eye drops. *J Pharm Pharmacol* 59, 629–635, doi:10.1211/jpp.59.5.0002 (2007). [PubMed: 17524227]
44. Ohira A et al. Topical dexamethasone gamma-cyclodextrin nanoparticle eye drops increase visual acuity and decrease macular thickness in diabetic macular oedema. *Acta Ophthalmol* 93, 610–615, doi:10.1111/aos.12803 (2015). [PubMed: 26201996]
45. Gilger BC *Ocular pharmacology and toxicology*. (Humana Press; Springer, 2014).
46. Ruiz-Ederra J et al. The pig eye as a novel model of glaucoma. *Exp Eye Res* 81, 561–569, doi:10.1016/j.exer.2005.03.014 (2005). [PubMed: 15949799]
47. Olsen TW, Aaberg SY, Geroski DH & Edelhauser HF Human sclera: thickness and surface area. *American journal of ophthalmology* 125, 237–241 (1998). [PubMed: 9467451]
48. Vurgese S, Panda-Jonas S & Jonas JB Scleral thickness in human eyes. *PLoS One* 7, e29692, doi:10.1371/journal.pone.0029692 (2012). [PubMed: 22238635]
49. Olsen TW, Sanderson S, Feng X & Hubbard WC Porcine sclera: thickness and surface area. *Investigative ophthalmology & visual science* 43, 2529–2532 (2002). [PubMed: 12147580]
50. Struble C, Howard S & Relph J Comparison of ocular tissue weights (volumes) and tissue collection techniques in commonly used preclinical animal species. *Acta Ophthalmol* 92, doi:10.1111/j.1755-3768.2014.S005.x (2014).
51. Rajapaksa TE et al. Intranasal M Cell Uptake of Nanoparticles Is Independently Influenced by Targeting Ligands and Buffer Ionic Strength. *J Biol Chem* 285, 23739–23746, doi:10.1074/jbc.M110.126359 (2010). [PubMed: 20511224]
52. Ensign LM, Hoen TE, Maisel K, Cone RA & Hanes JS Enhanced vaginal drug delivery through the use of hypotonic formulations that induce fluid uptake. *Biomaterials* 34, 6922–6929, doi:10.1016/j.biomaterials.2013.05.039 (2013). [PubMed: 23769419]
53. Pihl L, Wilander E & Nylander O Comparative study of the effect of luminal hypotonicity on mucosal permeability in rat upper gastrointestinal tract. *Acta Physiol (Oxf)* 193, 67–78, doi:10.1111/j.1748-1716.2007.01777.x (2008). [PubMed: 18005215]
54. Noach ABJ et al. Effect of Anisotonic Conditions on the Transport of Hydrophilic Model Compounds across Monolayers of Human Colonic Cell-Lines. *J Pharmacol Exp Ther* 270, 1373–1380 (1994). [PubMed: 7523659]
55. Nance EA et al. A Dense Poly(Ethylene Glycol) Coating Improves Penetration of Large Polymeric Nanoparticles Within Brain Tissue. *Science Translational Medicine* 4, 149ra119–149ra119, doi:10.1126/scitranslmed.3003594 (2012).
56. Wilhelmus KR The Draize eye test. *Survey of Ophthalmology* 45, 493–515, doi:10.1016/S0039-6257(01)00211-9 (2001). [PubMed: 11425356]
57. Wolffsohn JS et al. TFOS DEWS II Diagnostic Methodology report. *Ocul Surf* 15, 539–574, doi:10.1016/j.jtos.2017.05.001 (2017). [PubMed: 28736342]
58. Bron AJ, Evans VE & Smith JA Grading of corneal and conjunctival staining in the context of other dry eye tests. *Cornea* 22, 640–650 (2003). [PubMed: 14508260]

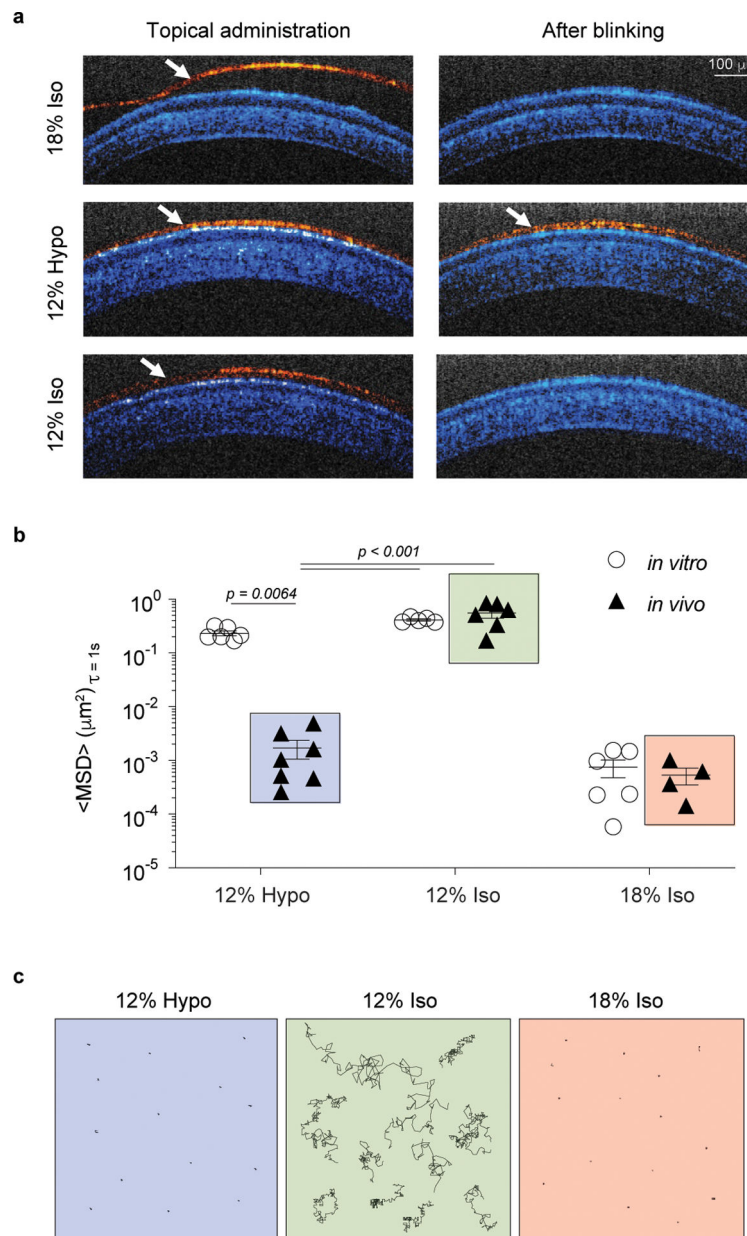


Fig 1 |. Hypotonicity drives water absorption that leads to uniform ocular surface coating and gelation.

a, Representative optical coherence tomography (OCT) images from rat eyes taken immediately after topical application (Left) of 12% Hypo, 12% Iso, and 18% Iso eye drops and after manually blinking the eyelids (Right). Images are false-colored to differentiate the eye structures (blue) and the topical formulations (red), $n = 5 - 6$ independent eyes and three images were obtained per eye. White arrows point to the eye drop layer. Scale bar = 100 μm and applies to all images. **b**, Ensemble averaged mean square displacement ($\langle \text{MSD} \rangle$) of 200 nm nanoparticles in various liquids and gels at 37°C *in vitro* and after application *in vivo* (particles visualized *ex vivo*). Each data point represents the ensemble average of 50 – 100 nanoparticles tracked in an individual sample, $n = 4 - 7$ independent animals. Data represented as the mean \pm SEM. Statistical analyses conducted by one-way ANOVA with

multiple comparisons with respect to the 12% Hypo *in vivo* group. The *in vivo* data groups with boxes around them correspond to those shown in c. **c**, Representative schematics showing the *ex vivo* tracked trajectories (~20 s) of nanoparticles in the 12% Hypo (Left) formulation compared with 12% Iso (Middle) and 18% Iso (Right) after ocular application *in vivo*.

Author Manuscript

Author Manuscript

Author Manuscript

Author Manuscript

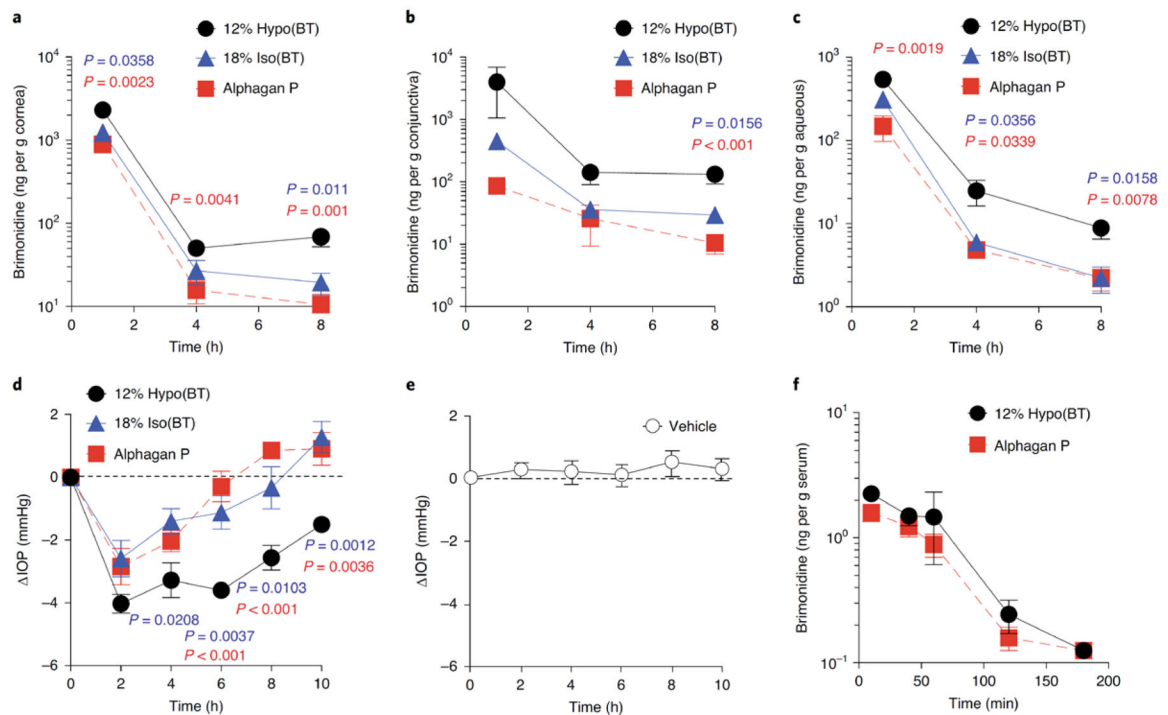


Fig 2 | Hypotonic gelling formulation (12% hypo) provides increased intraocular absorption of water-soluble BT (0.15% w/v) compared with the conventional gelling formulation (18% iso) or the commercially available formulation (Alphagan P).

a-c, BT concentrations in the rat cornea (**a**), conjunctiva (**b**) and aqueous humor (**c**) measured at 1, 4, and 8 h after the last dose (twice-daily dosing for 5 d, $n = 5-9$ independent animals). **d,e**, Change in IOP (Δ IOP) in normotensive rabbits measured for 10 h after a single dose comparing 12% hypo(BT) with 18% iso(BT) or Alphagan P (**d**) and the 12% hypo vehicle alone (Vehicle) (**e**) ($n = 5-6$ independent animals). Data are mean \pm s.e.m. Dotted lines mark the starting average IOP (Δ IOP = 0). **f**, BT concentrations in rabbit serum for up to 3 h after a single dose ($n = 4$ independent animals). Data are mean \pm s.e.m. Statistical analyses conducted by one-way ANOVA with multiple comparisons.

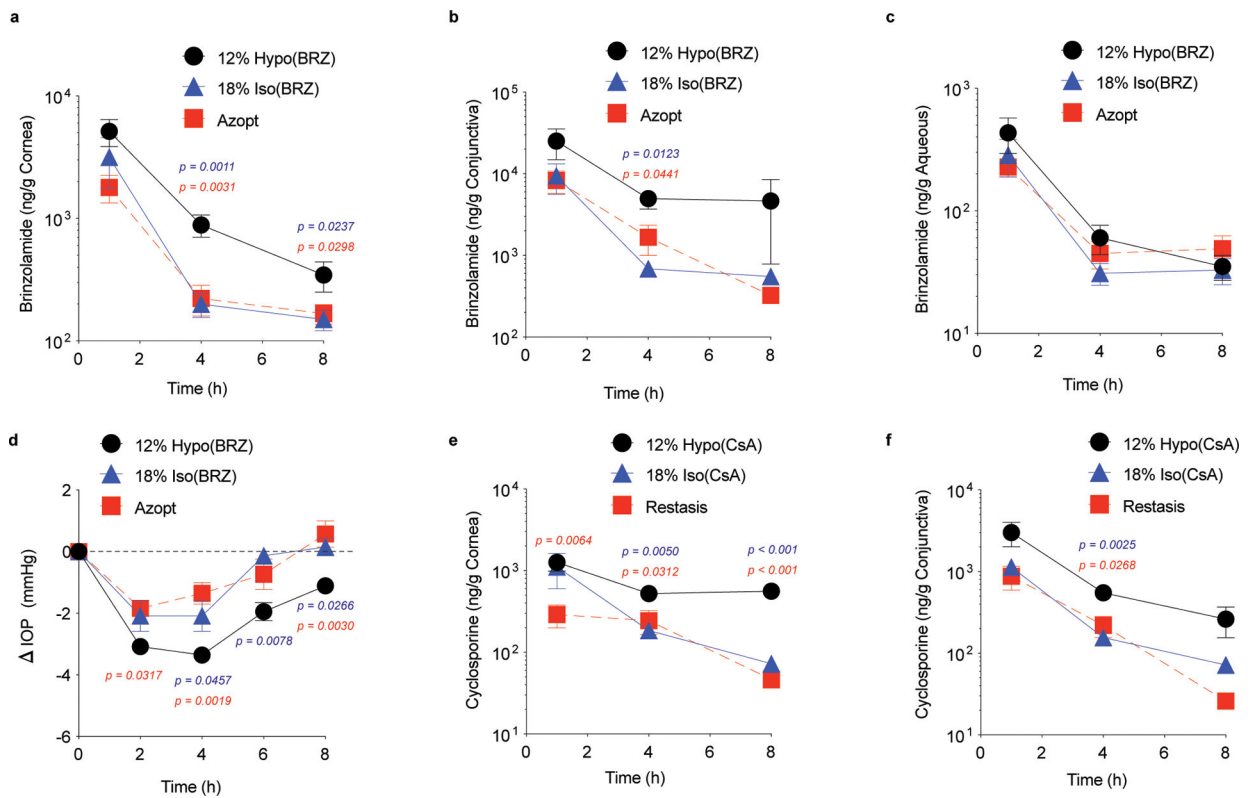


Fig 3 | Hypotonic gelling formulation (12% Hypo) solubilizes and provides improved intraocular delivery of two insoluble drugs, brinzolamide (BRZ, 1% w/v) and cyclosporine A (CsA, 0.05% w/v), compared to the conventional gelling formulation (18% Iso) or the commercially available formulations (Azopt®, Restasis®).

Brinzolamide concentrations in the rat (a) cornea, (b) conjunctiva, and (c) aqueous measured at 1, 4 and 8 h after the last dose (twice-daily dosing for 5 days, $n = 5 - 10$ independent animals). Change in intraocular pressure (Δ IOP) in normotensive rabbits measured for 8 h after a single dose, comparing (d) 12% Hypo(BRZ) to 18% Iso(BRZ) or to Azopt ($n = 5 - 6$ independent animals). Data shown as mean \pm SEM. Dotted lines mark the starting average IOP (Δ IOP = 0). CsA concentrations in the rat (e) cornea and (f) conjunctiva measured at 1, 4, and 8 h after the last dose (twice-daily dosing for 5 days, $n = 6 - 9$ independent animals). Statistical analyses conducted by one-way ANOVA with multiple comparisons.

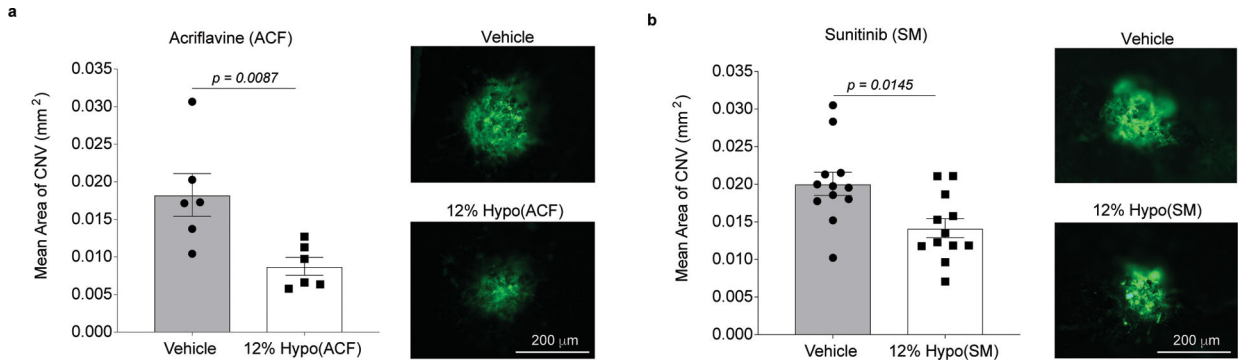


Fig. 4 |. Once-daily dosing of the hypotonic gelling formulation (12% Hypo) containing water-soluble acriflavine hydrochloride (ACF, 0.5% w/v) and sunitinib malate (SM, 0.4% w/v) in mice suppresses laser-induced choroidal neovascularization (CNV).

Laser-induced rupture of Bruch's membrane was performed in both eyes, and each mouse received the drug-containing drop in one eye and the 12% Hypo vehicle (Vehicle) in the contralateral eye immediately after laser and once per day thereafter (total 7 days). Both (a) 12% Hypo(ACF) (n = 6 independent eyes, one image was obtained per CNV spot) and (b) 12% Hypo(SM) (n = 12 independent eyes, one image was obtained per CNV spot) provided a significant reduction in the mean area of CNV. Data shown as mean \pm SEM. Statistical analyses conducted by a two-tailed Mann-Whitney test. Right panels show fluorescent images of CNV spots with areas representative of the means for each group. Scale bar = 200 μ m and applies to all images.

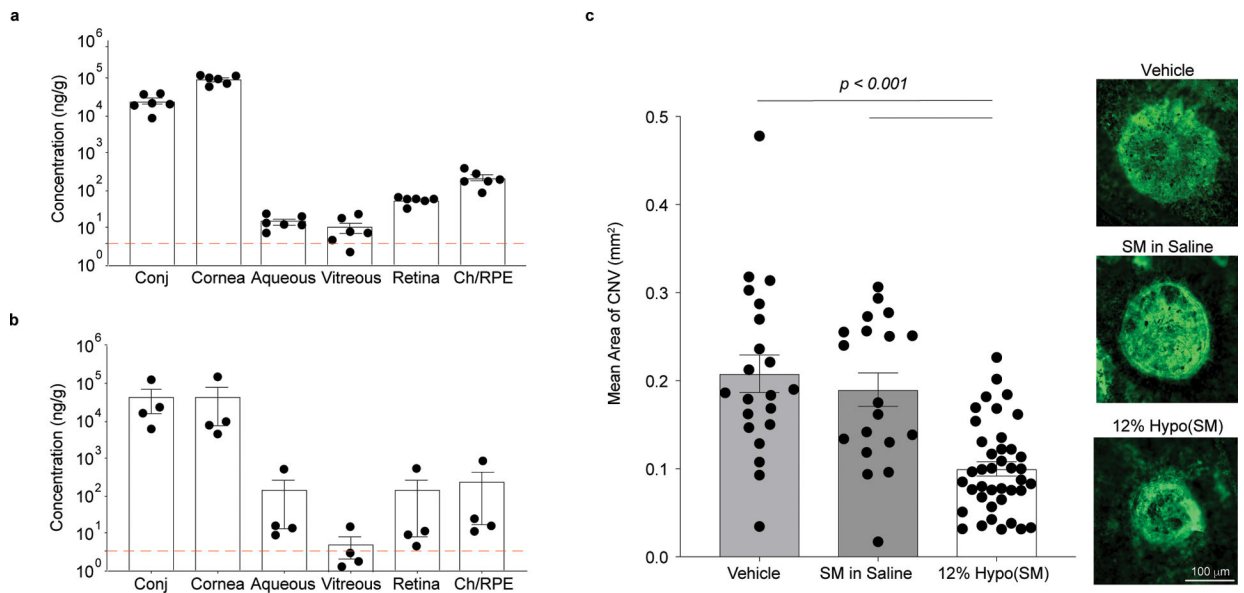


Fig 5 | Hypotonic gelling formulation (12% Hypo) provides therapeutically relevant delivery of sunitinib malate (SM, 0.4% w/v) to the posterior segment with once-daily dosing in rabbits and pigs.

a, Dutch belted rabbits were dosed unilaterally with 12% Hypo(SM) once daily for 14 days. Ocular tissues were collected 6 h after the last dose ($n = 6$ independent animals). Combined levels of sunitinib and N-desethyl sunitinib are shown with a dotted line indicating the K_i for VEGFR/PDGFR. **b**, Juvenile Yorkshire pigs received 12% Hypo(SM) once daily for 5 days unilaterally. Ocular tissues were collected 1 h after the last dose ($n = 4$ independent eyes). Combined levels of sunitinib and N-desethyl sunitinib are shown with a dotted line indicating the K_i for VEGFR/PDGFR. Drug concentrations achieved in the retina and choroid/retinal pigmented epithelium (Ch/RPE) exceed the inhibitory concentration. **c**, Laser-induced rupture of Bruch's membrane was performed in Juvenile Yorkshire pigs and each pig received either 12% Hypo(SM), SM dissolved in saline (SM in Saline), or 12% Hypo vehicle (Vehicle) bilaterally. Topical eye drops were given daily for a total of 15 days. Right panels show fluorescent images of CNV spots with areas representative of the means for each group. Scale bar = 100 μ m and applies to all images. The 12% Hypo(SM) ($n = 40$ CNV spots and one image was obtained per CNV spot) provided a significant reduction in mean area of CNV compared to 12% Hypo vehicle (Vehicle) ($n = 21$ CNV spots and one image was obtained per CNV spot) or SM in Saline ($n = 19$ CNV spots and one image was obtained per CNV spot). Statistical analyses conducted by linear mixed model. Data shown as mean \pm SEM.

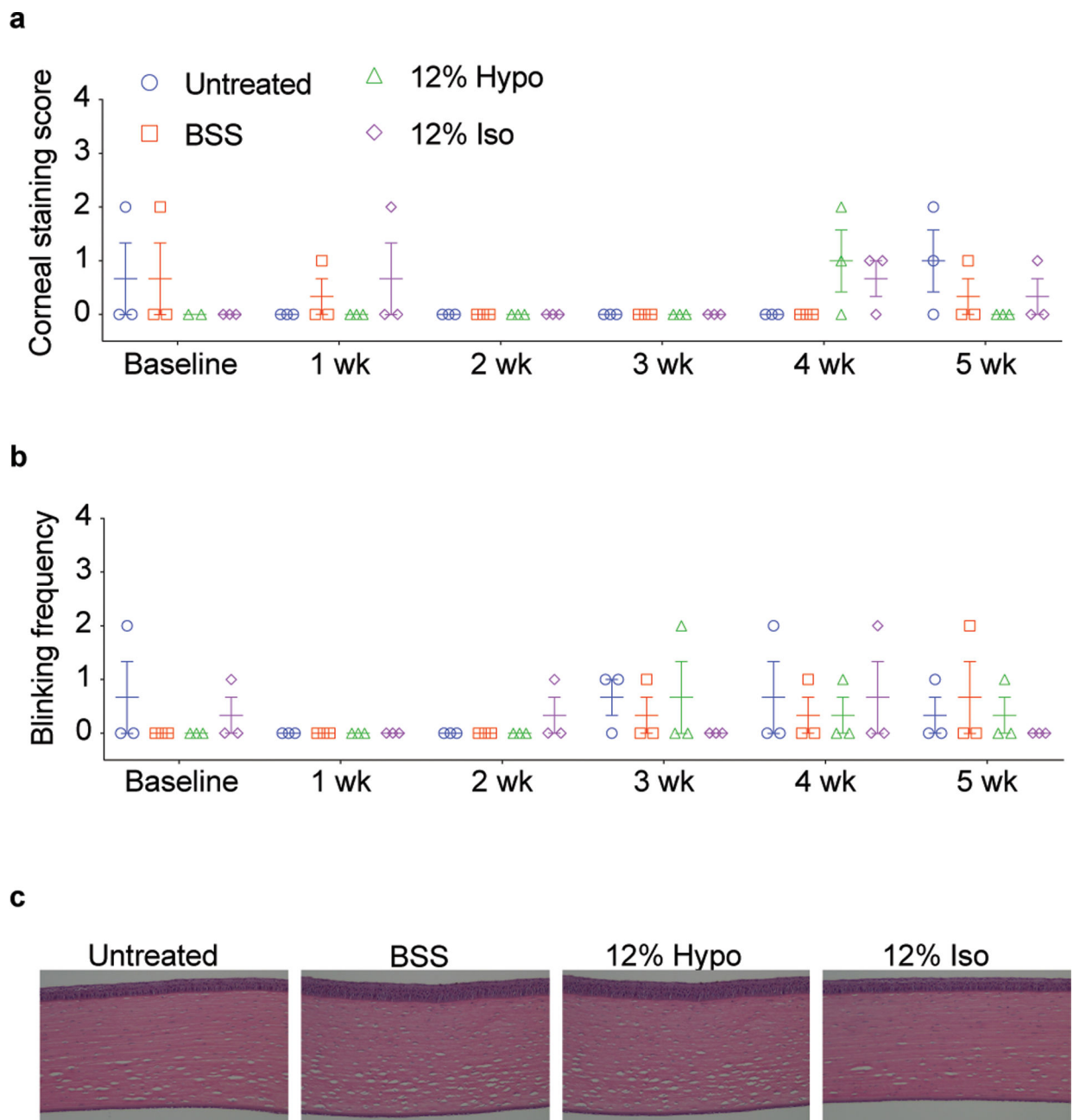


Fig 6 | Hypotonic gelling formulation (12% Hypo) is indistinguishable from no treatment (Untreated) with twice-daily dosing for 5 weeks in rabbits.

12% Hypo was compared to an isotonic formulation (12% Iso), isotonic balanced salt solution (BSS) and no treatment (Untreated) with bilateral administration of twice-daily dosing for 5 weeks in rabbits. Ocular surface damage, as assessed by (a) lissamine green staining and scoring and (b) counting the number of blinks in a 3 min period 3 h after the first dose on a given day, as well as (c) H&E staining of cornea tissues collected at 5 weeks (n = 3 independent eyes and one image was obtained per group), was indistinguishable across all groups.